



Smart bioelectronic pacifier for real-time continuous monitoring of salivary electrolytes

Hyo-Ryoung Lim ^{a,1}, Soon Min Lee ^{b,1}, Sehyun Park ^{c,d,1}, Chanyeong Choi ^{d,e}, Hojoong Kim ^{d,e}, Jihoon Kim ^{d,e}, Musa Mahmood ^{d,e}, Yongkuk Lee ^f, Jong-Hoon Kim ^{c,**}, Woon-Hong Yeo ^{d,e,g,h,*}

^a Major of Human Biocvergence, Division of Smart Healthcare, College of Information Technology and Convergence, Pukyong National University, Busan, 48513, Republic of Korea

^b Department of Pediatrics, Gangnam Severance Hospital, Yonsei University College of Medicine, Seoul, 06273, Republic of Korea

^c School of Engineering and Computer Science, Washington State University, Vancouver, WA, 98686, USA

^d IEN Center for Human-Centric Interfaces and Engineering at the Institute for Electronics and Nanotechnology, Georgia Institute of Technology, Atlanta, GA, 30332, USA

^e George W. Woodruff School of Mechanical Engineering, Georgia Institute of Technology, Atlanta, GA, 30332, USA

^f Department of Biomedical Engineering, Wichita State University, Wichita, KS, 67260, USA

^g Wallace H. Coulter Department of Biomedical Engineering, Georgia Tech and Emory University, Atlanta, GA, 30332, USA

^h Neural Engineering Center, Institute for Materials, Institute for Robotics and Intelligent Machines, Georgia Institute of Technology, Atlanta, GA, 30332, USA

ARTICLE INFO

Keywords:

Non-invasive monitoring
Salivary electrolyte
Bioelectronic pacifier
Capillary reservoir
Ion-selective electrode

ABSTRACT

Monitoring electrolytes is critical for newborns and babies in the intensive care unit. However, the gold standard methods use a blood draw, which is painful and only offers discrete measures. Although salivary-based detection offers promise as an alternative, existing devices are ineffective for real-time, continuous monitoring of electrolytes due to their rigidity, bulky form factors, and lack of salivary accumulation. Here, we introduce a smart, wireless, bioelectronic pacifier for salivary electrolyte monitoring of neonates, which can detect real-time continuous sodium and potassium levels without a blood draw. The miniature system facilitates the seamless integration of the ultralight and low-profile device with a commercial pacifier without additional fixtures or structural modifications. The portable device includes ion-selective sensors, flexible circuits, and microfluidic channels, allowing simplified measurement protocols in non-invasive electrolyte monitoring. The flexible microfluidic channel enables continuous and efficient saliva collection from a mouth. By modifying the surface properties of the channels and the structure of the capillary reservoir, we achieve reliable pumping of the viscous medium for quick calibration and measurement. Embedded sensors in the system show good stability and sensitivity: 52 and 57 mV/decade for the sodium and potassium sensor, respectively. In vivo study with neonates in the intensive care unit captures the device's feasibility and performance in the natural saliva-based detection of the critical electrolytes without induced stimulation.

1. Introduction

Over 480,000 ill children, including newborns, receive intensive care each year in the United States (Bonner et al., 2017; Wheeler and Wong, 2007; Xu et al., 2018). Children admitted to the neonatal intensive care unit (NICU) often require prolonged hospitalization due to their special health care needs caused by premature birth, low birth weight, or health conditions (Lean et al., 2018). Continuous monitoring of critical vital

signs, such as heart rate (HR), respiration rate (RR), temperature, blood oxygen level (SpO_2), blood pressure, and blood ion level, is crucial to preventing deterioration of health conditions and bringing resources in an efficient way for patient care. For example, it is known that the blood sodium level (135–145 mM/L) is related to blood pressure and heart failure, and the blood potassium level (3.6–5.2 mM/L) is associated with stroke (Green et al., 2002; Shea et al., 2008). However, most existing systems require a bulky, wall-tethered electronic processing unit,

* Corresponding author. IEN Center for Human-Centric Interfaces and Engineering at the Institute for Electronics and Nanotechnology, Georgia Institute of Technology, Atlanta, GA, 30332, USA.

** Corresponding author.

E-mail addresses: jh.kim@wsu.edu (J.-H. Kim), wheyo@gatech.edu (W.-H. Yeo).

¹ Equal contributions.



including multiple wired electrodes and sensor interfaces attached to the skins with adhesives. Even worse, regular blood testing is required. As a result, these monitoring systems could damage their vulnerable skin or induce other serious complications such as thrombus formation, blood vessel occlusion, sepsis, rupture, bleeding, and death (Baserga et al., 2002; Cilley, 1992; Joseph et al., 1985). Thus, a non-invasive health monitoring system of vital signs can improve the safety and effectiveness of health care in the NICU.

A fully wireless alternative that does not impose mechanical stress and potential injury risk is urgently needed to enhance the conventional standard of care. There have been many breakthroughs in wireless monitoring of physiological signals. However, little research explored blood ion level monitoring for babies (Lim et al. 2020, 2021a) since it is challenging to detect blood-related information underneath the skin. Several studies have demonstrated a positive correlation between blood and salivary ion levels via optical detectors. However, these devices require a rigid, bulky sensing component and additional supporting devices. For example, an integrated circuit, combined either with optical (Xu, 2021; Xu et al., 2019) or electrochemical field effect transistor system (Esashi and Matsuo, 1978), has a fragile part from a silicon wafer that could involve harmful health consequences in continuous monitoring. To address the issues of contemporary sensor systems, a miniaturized, potentiometric solid-state ion-selective electrode (SS-ISE) has been adopted as a good solution. The developed SS-ISE has successfully replaced fragile components of the conventional electrodes, and allowed for the miniaturization of the sensor's size (Hu et al., 2016). However, typical SS-ISEs have an intrinsic instability upon repetitive drying and stretching (Lopez et al., 2018). The film-type ion sensors also need a relatively wider surface for contacting the analyte for reliable signals. Especially for newborns in the NICU, accuracy is of prime importance to health professionals and caregivers due to the inability of the infants to express their discomfort or illness.

Recently, wearable physiological monitors and glucose detectors have been developed for babies, yet detecting ions still relies on blood measurements. More importantly, studies using SS-ISEs often overlook the correlation between blood and salivary ions, which raises questions about the validity of continuous and non-invasive monitoring. In salivary monitoring, ion levels depend on the sampling methods, sampling sites of interest (i.e., glands), and environmental conditions (Bellagambi et al., 2020; Jasim et al., 2016b; Williamson et al., 2012). For consistent results, it is imperative to standardize methods of supplying fresh saliva to the ion sensor surface. Although our prior studies (Lim et al. 2020, 2021a) show potential, this device still requires manual saliva collection, hindering real-time, continuous monitoring. To collect the saliva easier, one study integrated a wireless glucose sensor in a pacifier (Garcia-Carmona et al., 2019). However, this rigid and bulky system requires additional fixtures to press the pacifier, hindering natural saliva collection and adding mechanical burdens to the subject.

Here, we present a low-profile, portable, wireless, bioelectronic system for salivary electrolyte monitoring, which can detect the variation of sodium and potassium levels in real-time. This study includes a needle-type sensor that can fit into a much narrower space, such as the microfluidic channel structure. The miniaturized ion sensor, fabricated with thin metal wires, is then embedded in a small inner wall of a commercial pacifier. The overall system is flexible in a small form factor, such that it can be seamlessly attached to a pacifier without additional supporting components or structural modification. The microfluidic channel continuously suctions the saliva from a subject's mouth, enabling real-time monitoring of electrolytes. A specific pattern in the channel maximizes the capillary action against the viscous saliva, securely fixing the sensitive ion sensors in the channel reservoir. Moreover, the microfluidic channel stays hydrophilic at least seven days after oxygen plasma treatment by adding polydimethylsiloxane-polyethylene glycol (PDMS-PEG). The bioelectronic system exploits a low-energy Bluetooth module appropriate for long-term, continuous monitoring of target ions. In vivo study with infants demonstrates the

device's performance in continuous salivary electrolyte monitoring from unstimulated saliva. This study can provide evidence for the non-invasive, wireless, continuous, real-time, and easily assessable infant saliva diagnosis.

2. Materials and Methods

In this work, we present design strategies for developing a smart pacifier bioelectronics. This device consists of a Bluetooth-embedded circuit and a sensor-integrated microfluidic channel. The ion sensors in the system are metal conductors covered with appropriate polymer membranes, all of which are seamlessly integrated with a baby pacifier. The following is the detailed experimental protocols used in the development of devices.

2.1. General materials used for devices

Sodium tetrakis-[3,5-bis(trifluoromethyl)phenyl] borate (NaTFPB) was purchased from Alfa Aesar. 4-tert-Butylcalix [4] arene-tetraacetic acid tetraethyl ester (sodium ionophore X), bis(2-ethylhexyl)sebacate (DOS), poly(vinyl chloride) (PVC), tetrahydrofuran (THF), potassium tetrakis(p-chlorophenyl)borate(KTCIPB), hydrochloric acid (HCl), Ag wire, Nafion, Trichloro(1H,1H,2H,2H-perfluoroctyl)silane and polyvinyl butyral (PVB) were purchased from Sigma Aldrich. Sodium chloride, potassium chloride, calcium chloridedihydrate, and magnesium chloride hexahydrate were from Fisher Chemical. Ecoflex 00–30 was purchased from Smooth-On, and carbon black (CB, Vulcan XC 72R) was obtained from FuelCellStore. PDMS-PEG block copolymer (BCP) (DBE-712) was purchased from Gelest. Medical grade epoxy adhesive was purchased from Epoxy International.

2.2. Flexible circuits

Three ion electrodes were integrated with a flexible circuit. The circuit design followed the prior works (Lim et al., 2020; Mahmood et al., 2019), including a Bluetooth low-energy chip, a 2.45 GHz chip antenna, and a rechargeable battery. The flexible circuit was used to detect potential differences between the working electrode (WE) and a reference electrode (RE). The measured data was wirelessly transmitted to monitoring devices, such as tablets or smartphones.

2.3. Electrode fabrication

Ag wire was sonicated in an isopropyl alcohol (IPA) bath for 30 min. Ag wire was cut by 3 cm after the cleaning procedure. The CB/Ecoflex composite was prepared by mixing 6 wt% CB and 94% Ecoflex 00–30 in 15 g of toluene by stirring for 30 min at 600 rpm. After the mixing, the composite paste was dip-coated on the pre-cleaned Ag wire. Then, the CB/Ecoflex composite transducer was cured at 150 °C overnight. For the (RE), the Ag wire was chlorinated in a 0.1 M KCl and 0.01M HCl solution at 1 mA/cm² for 1 min.

2.4. Microfluidic channel fabrication

PDMS-PEG was purchased from Gelest (DBE-712) and exploited as an additive in the hydrophilic modification of the microfluidic channel. PDMS-PEG BCP was then added to the PDMS base, and the curing agent mix to obtain 1.0% (w/w). The mixture (PDMS + PDMS-PEG) was blended and poured onto a silicon wafer to cast the microfluidic channel. Trapped air bubbles were removed in a low-pressure desiccator. Before the casting process, the silicon wafer mold should be thoroughly salinized to enhance a clean release process. This process was done by incubating 2 µL droplet of trichlorosilane with the silicon wafer in a low-pressure desiccator overnight. Prepared PDMS-PEG was then poured over the wafer and cured in an oven at 70 °C for 24 h. Finally, the microfluidic channel structure was removed from the mold, and bonded

to a thin PDMS-PEG slab. The detailed procedure is described in the Supplementary Information.

2.5. Membrane fabrication

The CB/Ecoflex electrodes were coated with sodium or potassium ISM after complete drying. Two types of ISM were used; 1) sodium ISM: sodium ionophore X (2.67 mg), DOS (174.53 mg), PVC (88 mg), NaTFPB (1.47 mg) in 2 mL of THF (Wang et al., 2017), and 2) potassium ISM: KTFPB (0.8 mg), Valinomycin (2 mg), PVC (65.8 mg), DOS (131.4 mg) in 2 mL of THF (Guenat et al., 2006), respectively. The mixtures were vortexed for 6 h to make a homogeneous solution. The Ag/AgCl RE was coated with a membrane cocktail composed of 78.1 mg PVB, 50 mg KCl, and 1 mL methanol (Guinovart et al., 2014). The resulting ISEs and RE were dried at room temperature overnight.

2.6. Measurement of electrode sensitivity

Sodium chloride solutions with different concentrations were used to obtain the sensor information (10^{-3} to 0.1 M). Considering normal ion levels in human saliva (Sodium: 4–37 mM, Potassium: 2.6–18.3 mM), solutions with 10^{-3} to 0.1 M were used for repeatability and selectivity. For testing long-term repeatability and selectivity, we performed overnight conditioning and then initiating measurements (when the sensor was fully dried) and at least three times cleaning upon repetitive measurements to remove any residue from the sensor surface. The voltage response of all-solid-state ion ISE and a commercial RE (NT_MRX11) was performed. All sensor measurements were performed with a Gamry potentiostat (Interface 1010E, Gamry Instruments Inc).

2.7. System integration

Prepared ion sensors were embedded in the microfluidic channel. The gaps between the ion sensors and the channels were sealed with medical-grade epoxy adhesive and cured at room temperature for 24 h. A commercially available pacifier was purchased (Boon) and sterilized with ethylene oxide (EO) gas to ensure its biosafety (Mendes et al., 2007). The flexible circuit was attached to the pre-sterilized pacifier using medical-grade epoxy adhesive. After curing the epoxy, we integrated the microfluidic channel with ion sensors on the inner wall of the pacifier and connected them to the circuit pads via soldering.

2.8. Surface characterization of PDMS-PEG BCP

Water droplet contact angles were measured at the polymer sample. A contact angle goniometer (Ossila) was used to obtain the wettability performance of the PDMS-PEG BCP additive. 6 μ L of DI water was placed on the PDMS + PDMS-PEG BCP spin-coated glass slide, and the contact angle was measured at 5-min intervals to obtain the timeline data of surface arrangement. Wherever indicated, quantitative data were plotted as the mean \pm standard deviation ($n = 3$).

2.9. Human subject study

The study was conducted according to the guidelines of the approved IRB protocol (#3-2019-0206) from the Gangnam severance hospital at the Yonsei University College of Medicine. All subjects gave their informed consent.

3. Results and discussion

3.1. Overview of the system architecture and real-time ion monitoring mechanism

The presented work in this paper shows the smart pacifier's potential as a wearable non-invasive platform for continuous and real-time

monitoring of salivary ions in vivo. Fig. 1 captures the overall concept of non-invasive, real-time monitoring of salivary electrolytes via a smart bioelectronic pacifier. A pacifier consists of a flexible wireless circuit, a small microfluidic channel embedded with ion sensors, and a rechargeable battery (Fig. 1A). The flexible circuit is seamlessly attached to the backside of the pacifier. A detailed description of the low-power circuit and a list of chip components appear in Fig. S1 and Table S1. A couple of photos in Fig. 1B illustrates our target ions (sodium and potassium) and the saliva pathway. Specifically, the channel's end that is exposed at the back of the pacifier soaks up a baby's saliva for continuous flowing through the microchannels (Fig. 1C). As soon as the pacifier is inserted into the lip, saliva is suctioned through the channels. Then, continuous, and automatic feeding of fresh saliva is followed to a reservoir containing ion sensors. The detailed fabrication process of the smart pacifier system is described in Fig. S2 and Fig. S3. Overall, the device assembly follows multiple steps, including 1) fabrication of flexible circuits, ion sensors, and microfluidic channels, 2) integration of the sensors into the microfluidic structure, 3) attachment of the sensor-embedded channel and the circuit to the surface of a pacifier, and 4) final connection of the sensors and a rechargeable battery to the circuit pads via soldering. We also use the rechargeable battery with a magnetic connector for multiple uses (Fig. S4). The flow chart in Fig. 1D illustrates our method for continuous ion monitoring wirelessly. The voltage difference between a reference electrode and two SS-ISEs is measured and recorded by a mobile device with data filtering to suppress random noise signals. A schematic diagram in Fig. 1E compares our device's diagnostic and feedback protocols with the conventional table-top system, emphasizing the significance of the all-in-one, wearable, portable smart pacifier.

3.2. Design of microfluidic channels

Fig. 2A shows the key components to construct a smart pacifier, while Fig. 2B describes a layer-by-layer structure of the embedded microfluidic channel. The channel includes a PDMS-PEG layer, ion sensors, a capillary reservoir, and a PDMS-PEG base layer. The reservoir consists of capillary patterns grouped in multi-lines to fill the gap between the sensors. All designs on the top layers are 500 μ m in depth. One of the key advantages of our smart pacifier is the continuous saliva transportation that obviates the need for conventional discrete and manual sampling. While there have been many prior works regarding PDMS channels (Choi et al., 2017; Martín et al., 2017), the baby saliva analysis in this work has significant challenges; 1) Saliva has much more viscous than other biofluids such as sweat, 2) The microfluidic channel should be capable of transporting saliva in vertical position. This position is the way the gravity takes effect directly against the capillary effect, 3) The surface of the ion sensors must stay wet during the monitoring, and 4) PDMS is intrinsically a hydrophobic material that hamstrings the capillary effect. To resolve these challenges, we use PDMS-PEG and capillary pattern designs. The detailed procedure for analyzing the capillary force is described in Supplementary Note S1.

Table 1 summarizes recently reported biofluid monitoring devices that exploit PDMS microfluidic channels. It is well known that PDMS surfaces exposed to oxygen plasma become hydrophilic, and three or four oxygen atoms are bonded to silicon atoms, which reduces hydrophobicity (Hettlich et al., 1991). The main disadvantage of this method is a hydrophobic recovery of PDMS (Fig. 2C). We add PDMS-PEG BCP (1% w/w) when mixing the base and curing agent of PDMS to make PDMS-PEG BCP modified PDMS (PDMS + PDMS-PEG BCP). The PDMS-PEG BCP additive self-assembles at the interface of PDMS to create a hydrophilic PEG layer when exposed to water (Gökaltun et al., 2019). We measured sessile drop water contact angles (WCA) to test the hydrophilicity over timescales. The graph in Fig. 2C shows the difference in initial contact angle between PDMS and PDMS-PEG BCP after oxygen plasma treatment. While the WCA of PDMS became above 100°, the WCA of PDMS-PEG BCP remained below 80° even after seven days

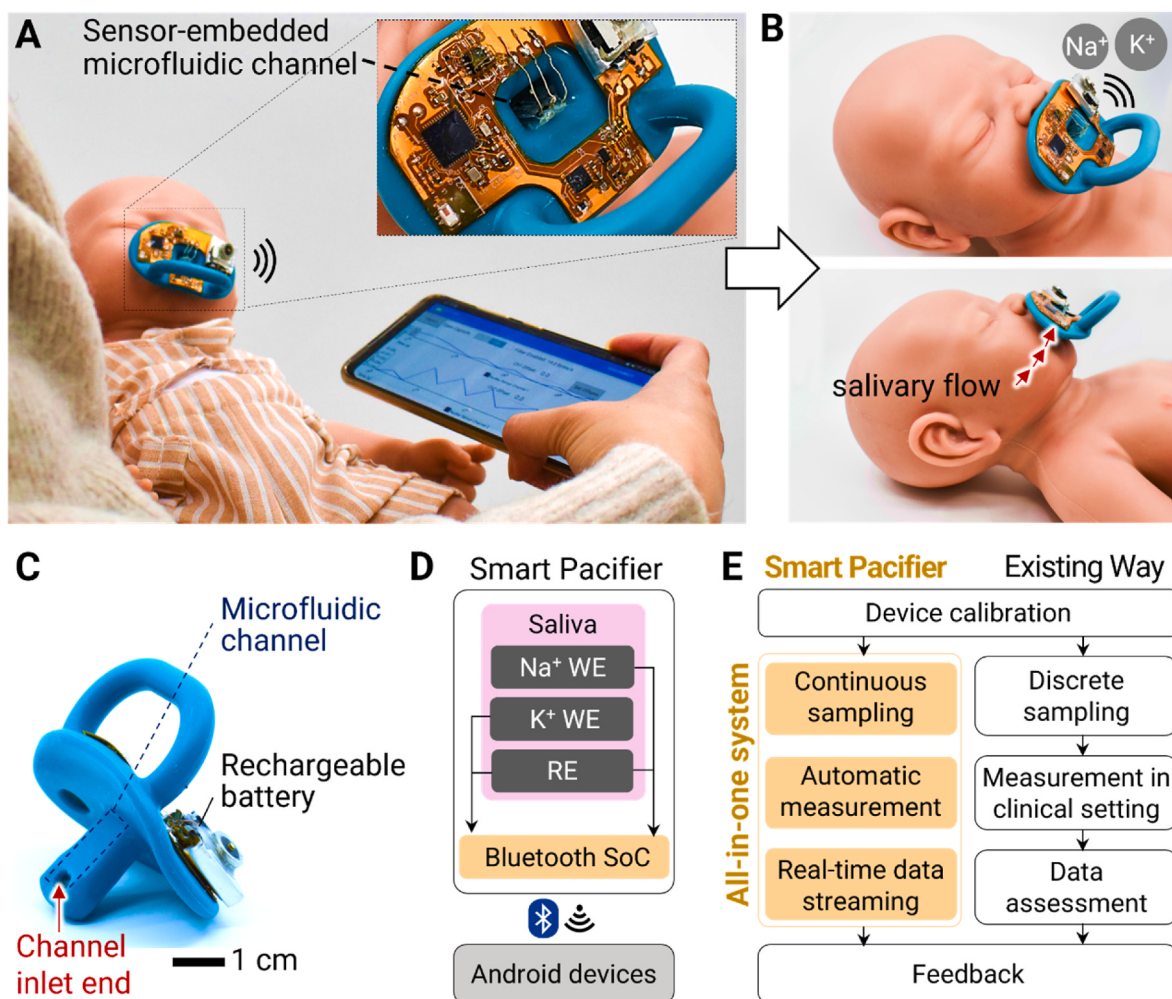


Fig. 1. Overview of designs and functions of a smart pacifier system for electrolyte monitoring. (A) A photo of a non-invasive, wireless sensor system integrated on a commercial pacifier, inserted into a baby model. The two-channel sensor signals detected in real time using a portable device. Inset: a photograph showing an enlarged view of the pacifier device composed of a flexible circuit and a microfluidic channel embedded with a sensor. (B) Photos of a worn pacifier at various angles, demonstrating its small, wearable design with a continuous salivary flow. (C) Side view that shows the locations of a microfluidic channel, an inlet end, and a rechargeable battery, delivering saliva and measuring ion concentration simultaneously. (D) Diagram capturing the key sensing components of the smart pacifier for a wireless data recording with a portable device. (E) Comparison of measurement protocols of our all-in-one smart pacifier with existing table-top devices.

(Table S2). Moreover, when it contacts water, PEG group rearrangement renders the surface hydrophilic. Fig. 2D shows decreasing of contact angle over time. When PDMS-PEG BCP was exposed to water, the WCA significantly reduced over time. Higher BCP-containing samples (1.5% and 2.0% PDMS-PEG BCP) showed more hydrophilicity. Nevertheless, the higher percentage of BCP made the samples much viscous before curing. It was too viscous for the trapped bubble to be removed from the samples after the molding step.

Epoxy adhesives are hydrophilic due to polar epoxy groups (Palanisamy et al., 2017). For bonding the microfluidic channel, we used a medical-grade epoxy adhesive. A stamping method was used to coat the epoxy adhesive on the microfluidic channel. After the slab was put on the microfluidic channel, an epoxy adhesive was squeezed into the microfluidic chamber. Then, the gaps between the slab and the channel were filled to make the edges where the channel and slab chamber meet hydrophilic. The function of the capillary patterns is to enhance the capillary force (Zimmermann et al., 2007) and prevent the collapse of the reservoir chamber (Martín et al., 2017). Next, we used the EO gas to sterilize a commercial pacifier to avoid harming baby subjects. Afterward, the sensor-embedded channel and flexible circuit were integrated onto the pre-sterilized pacifier (Fig. S5A). In this way, a subject is exposed only to a safe portion: a pre-sterilized pacifier and a

biocompatible PDMS inlet (Figs. S5B–C). Further, the two cm-long channel outlet was positioned at the back of the device (Fig. S5D) so that the used saliva barely reaches and affects the subject after measurement. The channel's ability to soak up fluid allows saliva to pass through in one direction without flowing backward (Fig. S6). Ultimately, our system minimized toxicity issues associated with sensors, circuits, or batteries through these processes. We also demonstrated the fluid-transporting capability of the microchannel in Fig. 2E and F with simulation results and experimental validation. An experimental demonstration of the fluid transporting performance appears in Supplementary Video S1. The testing fluid, a mixture of water and glycerin, was designed to be much more viscous (2 cP) than saliva, considering reported values (Govindaraj et al., 2019). The channel successfully transported the saliva vertically even without ion sensors. After the sensor was integrated into the microfluidic channel, the gap between the capillary patterns groups in the reservoir was filled by the ion sensors.

Supplementary data related to this article can be found at <https://doi.org/10.1016/j.bios.2022.114329>.

3.3. Characterization of ion sensors

Fig. 3 summarizes sensors' performance and characterization data.

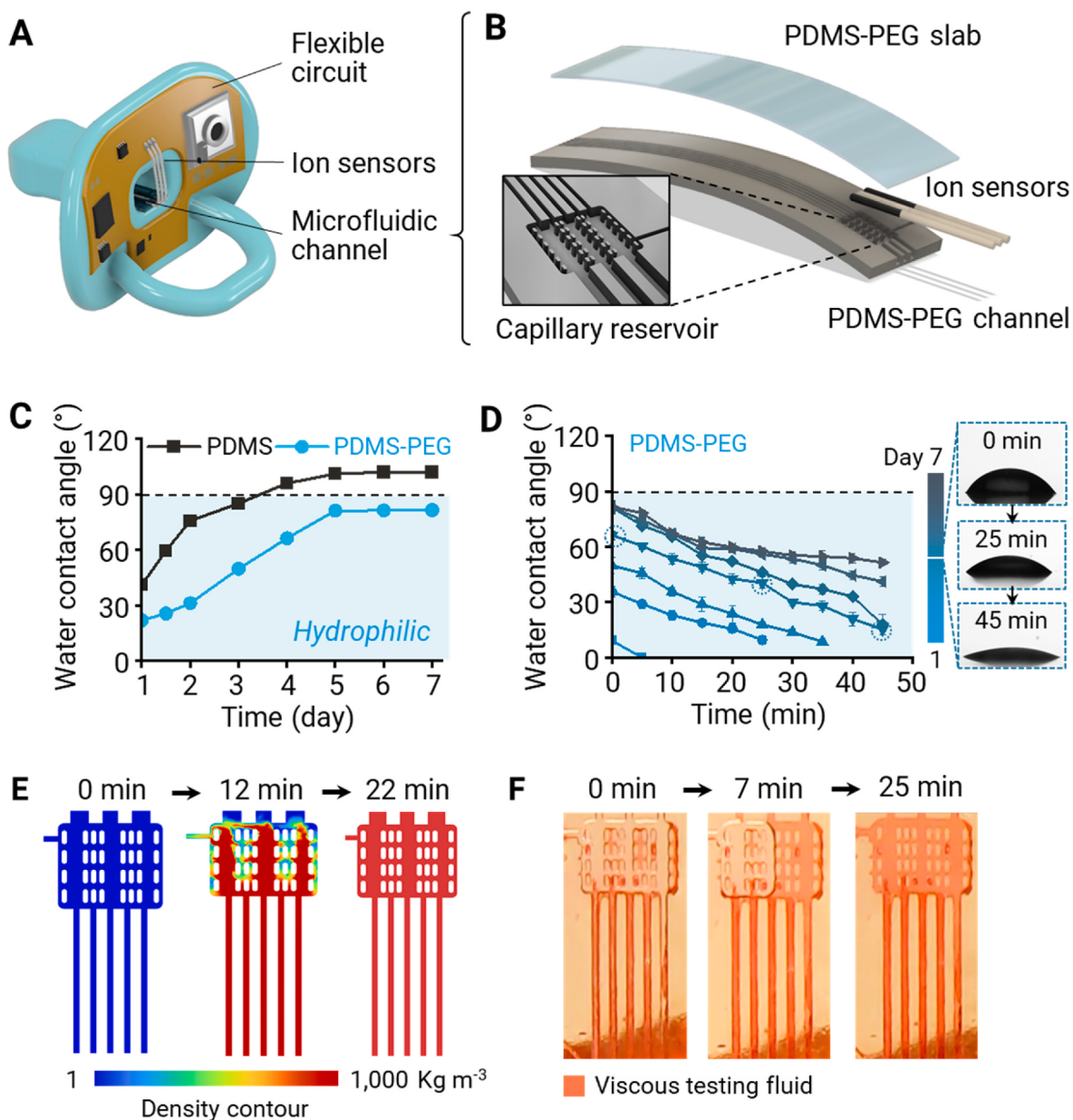


Fig. 2. Design and characterization of microfluidic channels. (A) Schematic illustration of a smart pacifier including microfluidic channels. (B) Exploded view of the detailed design of the channel with multiple components. (C) Comparison of water contact angles on PDMS and PDMS-PEG over time. (D) Changes of water contact angles on PDMS-PEG over time. Inset images show photos of contact angles at 0, 25, and 45 min on the surface. (E) Simulation results of fluid transport over time until the channel is filled. (F) Experimental demonstration of transporting performance of the microfluidic channel, showing a similar trend as estimated in (E).

We designed low-profile, wire-type ion sensors, consisting of a solid-state WE and a RE, which are seamlessly embedded into the prepared microfluidic channels. The detailed fabrication procedure of ion sensors and measurement setup appear in Fig. S7. The WEs of which ion-to-electron transducer is a composite of CB and Ecoflex were coated with sodium and potassium ion-selective membranes (Fig. S7A). Another silver wire sample was electrochemically chlorinated to coat a chemically stable surface of silver chloride. Subsequently, PVB/KCl and Nafion were coated to negate a dissolution of chloride ions and thus to avoid signal failures (Fig. S7B). In this work, we confirm the wire-type sensors' functionality. A table-top potentiometer was used to verify the functionality of ion-selective electrodes, compared with the measurement from our wireless system (Figs. S7C and S8, Table S3). A real-time voltage transient, measured by the potentiometer, appears in Fig. 3A and D. The sodium and potassium sensing electrodes show stable, repeatable, and rapid response to 10^{-3} , 10^{-2} , and 10^{-1} M NaCl and KCl

solutions, verifying the good functionality of our wire-type sensors. Their calculated sensitivity (52 mV/decade for sodium; 57 mV/decade for potassium ion sensors) confirms that the electrode response is close to the theoretical values according to the Nernst equation (Fig. 3B and E) (Ross, 1969). We also observed similar results when the other edge of the silver wire was soldered to the circuit of our smart pacifier designed to measure and transfer data wirelessly (Fig. S8). Voltage stability of sensors is critical to be used in clinical applications; low accuracy of SS-ISE due to an unwanted signal fluctuation is problematic (Tsunoda et al., 2015) (Fan and Andrew, 2020). We resolved the stability issue in this work, as demonstrated in Fig. 3C and F. The electrodes show long-term stability of 4.3 mV/h in NaCl solutions and 3 mV/h in KCl solutions for 10 h. The inset images in Fig. 3C and F displays an enlarged view of the voltage fluctuations for an hour, where standard deviation is 2.0 mV and 0.3 mV for each ion. The demonstrated stability of the sensors is noteworthy considering our device is designed to operate for

Table 1

Comparison of recently developed non-invasive devices that monitor biological fluids.

Reference	Device configuration	Target biofluid	Microfluidic channel		Sensor type	Wireless monitoring
			Hydrophilic treatment	Capillary pattern		
This work	All-in-one, integrated pacifier	Saliva	PDMS-PEG, O ₂ plasma	Yes	Wire-type	Yes
[1]	Flexible PCB	Sweat	No	No	Film-type	Yes
[3]	Rigid PCB	Sweat	No	No	Film-type	Yes
[5]	Rigid PCB	Sweat	No	No	Film-type	Yes
[6]	Rigid PCB	Sweat	No	No	Film-type	Yes
[12]	Rigid PCB	Sweat	No	No	Film-type	Yes
[11]	Rigid PCB	Sweat	O ₂ plasma	No	Film-type	Yes
[13]	Rigid PCB	Sweat	No	No	Film-type	Yes
[9]	Thin film PCB	Sweat	No	No	Film-type	Yes
[10]	–	Sweat	No	No	Film-type	No
[2]	–	Sweat	No	No	Film-type	No
[7]	–	Sweat	No	No	Film-type	No
[8]	–	Sweat	O ₂ plasma	No	Film-type	No
[4]	–	Sweat	No	No	Film-type	No

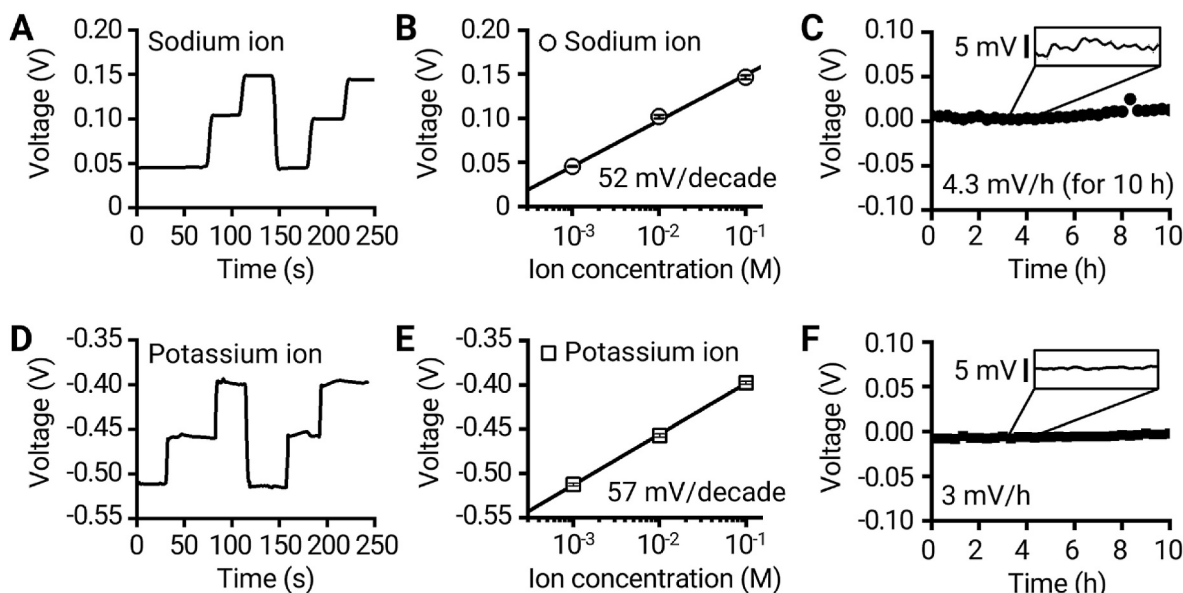


Fig. 3. Characterization of ion sensors. (A–B) Time-voltage transients measured with different NaCl solution concentrations (10^{-3} , 10^{-2} , and 10^{-1} M) and the sensitivity of the sodium ion sensor. (C) Voltage stability test of a sodium ion sensor for 10 h along with an enlarged inset for 1-h data. (D) Voltage signal recorded at 10^{-3} , 10^{-2} , and 10^{-1} M KCl solutions. (E) Calculated sensitivity of the potassium sensor. (F) Long-term stability test of the sensor for 10 h (inset: an-hour voltage transients).

multiple hours. Furthermore, the results validate the electrodes' structures with particular emphasis on their small wire-like form, which can be easily and seamlessly integrated with miniaturized fluidic channels.

3.4. In vivo study and demonstration of the device's performance

An example of our implemented medical use of a fabricated smart pacifier is shown in Fig. 4, which demonstrates the system's performance by comparing the data with the conventional blood-draw results. For this in vivo study, we used a commercially available pacifier to integrate our sensors and electronics (Fig. 4A). After sterilizing the pacifier, we integrated a flexible circuit, sensors, and microfluidic channels with minimal design changes. During the study, only the pre-cleaned area made an oral contact with subjects. In the wearable design of the pacifier, the use of typical pacifiers offers comfort to subjects (babies), while reducing manufacturing costs. Fig. 4B depicts a comparison between non-invasive (smart pacifier) and invasive (blood draw) measurements of ion concentrations in saliva and serum, respectively. Our wearable system provides real-time, continuous

monitoring of sodium and potassium ions from saliva for multiple hours. As of now, the electrolyte-based health monitoring in the NICU requires blood draws of babies at least twice daily from their feet, which typically causes bruises. More importantly, it is a single-point, discrete measurement that cannot provide real-time health information of sick babies. There are many types of ion sensors demonstrating great potential for better accuracy (Kalidoss et al., 2018), multimodal analysis (Onicescu et al., 2013; Urbanowicz et al., 2019), and flexible system (Bao et al., 2019). But the bulky structures limit to only use spitting saliva. Such system is insufficient to meet the needs for continuous sampling and analysis, especially for babies who cannot collect samples by themselves. Furthermore, the resulting electrolytes' levels are highly dependent on the measurement settings, including sampling sites, methods, and temperatures. These parameters may be neglected in discrete sampling methods. For example, the sodium ion concentrations in saliva vary from 5.6 mM (Urbanowicz et al., 2019) to 70 mM (Onicescu et al., 2013), limiting the clinical use of salivary diagnosis. In this study, our focus is on the importance of concurrent data collection and analysis, which would help achieve the ultimate goals of a wearable

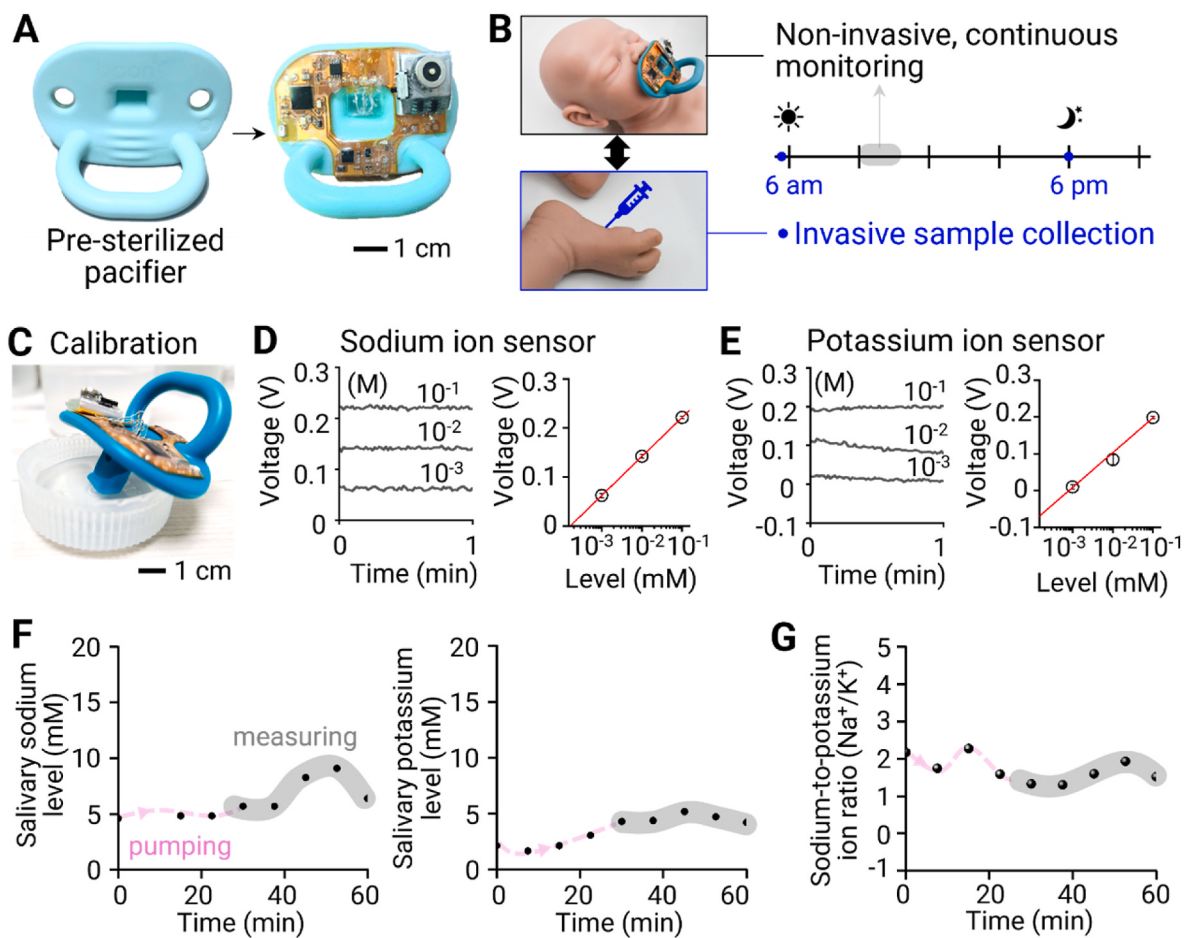


Fig. 4. In vivo study and demonstration of the device's performance. (A) Use of a commercial pacifier to sterilize, which is used to integrate other components with minimal modification. (B) Comparison of non-invasive, continuous monitoring method (smart pacifier) and the conventional invasive method. A blood sample is extracted from one foot at least twice a day. (C) Photo of the smart pacifier during calibration using a small sample volume (<5 mL). (D) Calibration result of the sensor with sodium ions with different concentrations. (E) Calibration result of the sensor for detecting potassium ions. (F) Sodium and potassium ion levels simultaneously recorded for an hour, demonstrating real-time and continuous monitoring. (G) Sodium-to-potassium ion ratio that is useful for prognosis and diagnosis of diseases such as cardiovascular disease risks.

healthcare monitor: (i) providing real-time data for immediate feedback, and (ii) expanding the field of non-invasive health monitoring.

A set of data in Fig. 4C–G demonstrates the novelty of unique advantage of the smart pacifier system in detection of sodium and potassium ions. We calibrated the sensors after conditioning using three different calibration solutions. Using a swab and blower, we reduced the calibration time by sucking the remaining solution in the channels (detailed protocol is described in the Materials and Methods section). As shown in Fig. 4C, we calibrated the system by using drops with a small volume (<5 mL) of 10^{-3} , 10^{-2} , and 10^{-1} NaCl and KCl solutions. By leaning the small container 45° , it was possible to capture clear signals due to the microfluidic channels' hydrophilic surfaces. Additionally, we increased the gain of voltage signals for improved measurement accuracy (Fig. 4D and E). Using an amplifier-circuit gain, the voltage value and sensitivity are multiplied by a circuit gain that can be adjusted by the user via a mobile app (Lee et al., 2018). In this case, when the gain was set to 1.5, the linearities for sodium and potassium ions sensors were 80 and 95 mV/decade, respectively. The sensitivity of these sensors has been calculated at 53 and 63 mV/decade, close to the Nernst level (59 mV/decade). The difference may arise as a result of differences in temperature (Zdrachek and Bakker, 2018), voltage stability of the reference electrode (Kalidoss et al., 2018), and biofouling on the surface of the sensors (Garcia-Carmona et al., 2019). Even though we must continue to improve the sensing capabilities in a future study, we believe that our gain adjustment method could increase the accuracy and

usability at the device level. Fig. 4F validates the wearable device's performance in continuous monitoring of salivary sodium and potassium. The measured data shows salivary concentrations of 5.7–9.1 mM for sodium (average value: 7.1 mM) and 4.2–5.2 mM for potassium (average value: 4.6 mM). These values are reasonable since they are within the known levels of salivary ions from prior works (4–37 mM for sodium; 3–18 mM for potassium) (Kallapur et al., 2013). Note that the low ion levels detected during the first 30 min may be attributed to a pumping effect since it takes up to 25 min for the viscous fluid to reach the sensors. The ratio of sodium to potassium levels is well known to be related to various health problems such as cardiovascular disease, chronic kidney disease, diabetes, and aldosteronism (Geleijnse et al., 2007; Kallapur et al., 2013; Laufer et al., 1962; Manley, 2014; Whelton, 2014). As shown in Fig. 4G, the smart pacifier measures the sodium-to-potassium ratio, which can be used to diagnose and prognosis diseases.

This work provides an insight into the important area of non-invasive salivary monitoring. Compared to our previous works that demonstrated a small, wireless, flexible ion sensor system (Lim et al. 2020, 2021b), the novelty of this new approach lies in creating an all-in-one feature that meets the challenges of developing fully automatic non-invasive protocols. The former methodology required users to gather a saliva sample—which may require medical personnel if the patients were infants—and to drop the sample on film electrodes in a discrete manner. Our new wearable device, to provide maximum user comfort and

practical efficiency, has been designed to simultaneously implement continuous sampling, auto measurement, and real-time data streaming. To validate the wearable device's accuracy, we previously reported a correlation with blood ions under discrete sampling conditions in clinical practice (Lim et al., 2021b): $y = 1.25x + 120.7$ where x is a sodium level in saliva and y is a sodium level in blood. By using this equation, the blood sodium level is calculated to be 130 mM in average, which is lower than the measured values (139 and 138 mM). The small discrepancy can be explained by the difference between discrete blood draws and continuous salivary detection, which may be affected by temperature, sampling procedures, and gland sites. For example, the well-known Nernst equation indicates that temperature has a significant effect on the resulting potential values (Bobacka et al., 2008; Lyu et al., 2020; Shao et al., 2020). Therefore, in clinical trial (e.g., urinary catheters), the use of temperature sensors is recommended to correct for body temperature differences between the bladder temperature and the equilibration temperature used to prepare the standards (Zdracheck and Bakker, 2018). Temperature is clearly an important factor; however, it is still too early to make any definite statements due to the presence of a number of variables to be considered (e.g., a difference in molecular levels between whole and accumulated saliva) (Jasim et al., 2016a). The main focus of this proof-of-concept study is the development of an all-in-one system for continuous electrolyte monitoring from saliva, while multimodal sensors along with an automatic compensation system should be investigated. Future work will conduct a large-group clinical study to standardize the salivary detection method for simplified, continuous, and real-time monitoring of electrolytes.

4. Conclusion

This paper reports a portable bioelectronic pacifier system, allowing for a wireless, real-time, continuous detection of sodium and potassium levels without a blood draw. For the first time, the miniaturized wearable system shows a reliable salivary electrolyte monitoring of neonates. In vivo study in the NICU demonstrated the device's capability of monitoring sodium (5.7–9.1 mM) and potassium (4.2–5.2 mM) levels continuously in real-time. The innovative flexible platform, consisting of a wireless circuit, surface-modified microfluidic channels, and SS-ISEs embedded in a capillary reservoir, together with a pacifier, could offer non-invasive neonatal health monitoring. To apply the study outcome to real-world settings, our future work will focus on conducting a large-group clinical study, while developing additional electrolyte sensors and repeatable sterilization protocols.

CRediT authorship contribution statement

Hyo-Ryoun Lim: Formal analysis, Writing – original draft, conceived and designed the research, performed the experiments, analyzed the data. **Soon Min Lee:** Conceptualization, Formal analysis, analyzed the data. **Sehyun Park:** Writing – original draft, performed the experiments. **Chanyeong Choi:** Experiment. **Hojoong Kim:** Experiment. **Jihoon Kim:** Experiment. **Musa Mahmood:** Experiment. **Yong-kuk Lee:** Experiment. **Jong-Hoon Kim:** Formal analysis, and analyzed the data. **Woon-Hong Yeo:** Conceptualization, Writing – original draft, conceived and designed the research, wrote the paper.

Declaration of competing interest

The authors declare the following financial interests/personal relationships which may be considered as potential competing interests: Georgia Tech has a pending US patent application.

Acknowledgements

We acknowledge the support of the "Mirae Medical" Faculty Research Assistance Program of Yonsei University College of Medicine

for (6-2020-0237) and the IEN Center Grant from the Georgia Tech Institute for Electronics and Nanotechnology. Electronic devices in this work were fabricated at the Institute for Electronics and Nanotechnology, a member of the National Nanotechnology Coordinated Infrastructure, which is supported by the National Science Foundation (grant ECCS-2025462).

Appendix A. Supplementary data

Supplementary data to this article can be found online at <https://doi.org/10.1016/j.bios.2022.114329>.

References

- Bao, G., Kaur, M., Kim, W.S., 2019. Sensor. Actuator. B Chem. 285, 186–192.
- Baserga, M.C., Puri, A., Sola, A., 2002. J. Perinatol. 22 (5), 416–419.
- Bellagambi, F.G., Lomonaco, T., Salvo, P., Vivaldi, F., Hangouét, M., Ghimenti, S., Biagini, D., Di Francesco, F., Fuoco, R., Errachid, A., 2020. Trac. Trends Anal. Chem. 124, 115781.
- Bobacka, J., Ivaska, A., Lewenstam, A., 2008. Chem. Rev. 108 (2), 329–351.
- Bonner, O., Beardsall, K., Crilly, N., Lasenby, J., 2017. BMJ innovations 3 (1).
- Choi, J., Kang, D., Han, S., Kim, S.B., Rogers, J.A., 2017. Adv. Healthcare Materials 6 (5), 1601355.
- Cilley, R., 1992. Semin. Pediatr. Surg. 1 (3), 174–180.
- Esashi, M., Matsuo, T., 1978. IEEE Transact. Biomed. Eng. BME- 25 (2), 184–192.
- Fan, R., Andrew, T.L., 2020. J. Electrochim. Soc. 167 (3), 37542.
- Garcia-Carmona, L., Martin, A., Sempionatto, J.R., Moreto, J.R., Gonzalez, M.C., Wang, J., Escarpa, A., 2019. Anal. Chem. 91 (21), 13883–13891.
- Geleijnse, J.M., Witteman, J., Stijnen, T., Kloos, M.W., Hofman, A., Grobbee, D.E., 2007. Eur. J. Epidemiol. 22 (11), 763–770.
- Gökaltun, A., Kang, Y.B.A., Yarmush, M.L., Usta, O.B., Asatekin, A., 2019. Sci. Rep. 9 (1), 1–14.
- Govindaraj, S., Daniel, M.J., Vasudevan, S.S., Kumaran, J.V., 2019. Dentistry Medical Res. 7 (2), 56.
- Green, D., Ropper, A., Kronmal, R., Psaty, B., Burke, G., 2002. Neurology 59 (3), 314–320.
- Guenat, O.T., Generelli, S., de Rooij, N.F., Koudelka-Hep, M., Berthiaume, F., Yarmush, M.L., 2006. Anal. Chem. 78 (21), 7453–7460.
- Guinovart, J.T., Crespo, G.A., Rius, F.X., Andrade, F.J., 2014. Anal. Chim. Acta 821, 72–80.
- Hettlich, H.-J., Otterbach, F., Mittermayer, C., Kaufmann, R., Klee, D., 1991. Biomaterials 12 (5), 521–524.
- Hu, J., Stein, A., Bühlmann, P., 2016. Trac. Trends Anal. Chem. 76, 102–114.
- Jasim, H., Olaussen, P., Hedenberg-Magnusson, B., Ernberg, M., Ghafouri, B., 2016a. Sci. Rep. 6 (1), 39073.
- Jasim, H., Olaussen, P., Hedenberg-Magnusson, B., Ernberg, M., Ghafouri, B., 2016b. Sci. Rep. 6, 39073.
- Joseph, R., Chong, A., Teh, M., Wee, A., Tan, K., 1985. Ann. Acad. Med. Singapore 14 (4), 576–582.
- Kalidoss, R., Sivantha Raja, A., Jeyakumar, D., Prabu, N., 2018. IEEE Sensor. J. 18 (20), 8510–8516.
- Kallapur, B., Ramalingam, K., Bastian Mujib, A., Sarkar, A., Sethuraman, S., 2013. J. Nat. Sci. Biol. Med. 4 (2), 341–345.
- Lauler, D.P., Hickler, R.B., Thorn, G.W., 1962. N. Engl. J. Med. 267 (22), 1136–1137.
- Lean, R.E., Rogers, C.E., Paul, R.A., Gerstein, E.D., 2018. Current treatment options in pediatrics 4 (1), 49–69.
- Lee, Y., Howe, C., Mishra, S., Lee, D.S., Mahmood, M., Piper, M., Kim, Y., Tieu, K., Byun, H.S., Coffey, J.P., Shayan, M., Chun, Y., Costanzo, R.M., Yeo, W.H., 2018. Proc. Natl. Acad. Sci. U. S. A. 115 (21), 5377–5382.
- Lim, H.-R., Kim, Y.-S., Kwon, S., Mahmood, M., Kwon, Y.-T., Lee, Y., Lee, S.M., Yeo, W.-H., 2020. Sensors 20 (11), 3297.
- Lim, H.-R., Lee, S.M., Mahmood, M., Kwon, S., Kim, Y.-S., Lee, Y., Yeo, W.-H., 2021a. Sensors 21 (5), 1642.
- Lim, H.-R., Lee, S.M., Mahmood, M., Kwon, S., Kim, Y.-S., Lee, Y., Yeo, W.-H., 2021b. Sensors 21 (5).
- Lopez, L., Kim, Y., Jierry, L., Hemmerle, J., Boulmedais, F., Schaaf, P., Pronkin, S., Kotov, N.A., 2018. ACS Nano 12 (9), 9223–9232.
- Lyu, Y., Gan, S., Bao, Y., Zhong, L., Xu, J., Wang, W., Liu, Z., Ma, Y., Yang, G., Niu, L., 2020. Membranes 10 (6).
- Mahmood, M., Mzurikwao, D., Kim, Y.-S., Lee, Y., Mishra, S., Herbert, R., Duarte, A., Ang, C.S., Yeo, W.-H., 2019. Nat. Mach. Intell. 1 (9), 412–422.
- Manley, K.J., 2014. J. Ren. Care 40 (3), 172–179.
- Martin, A., Kim, J., Kurniawan, J.F., Sempionatto, J.R., Moreto, J.R., Tang, G., Campbell, A.S., Shin, A., Lee, M.Y., Liu, X., 2017. ACS Sens. 2 (12), 1860–1868.
- Mendes, G.C.C., Brandão, T.R.S., Silva, C.L.M., 2007. Am. J. Infect. Control 35 (9), 574–581.
- Oncescu, V., O'Dell, D., Erickson, D., 2013. Lab Chip 13 (16), 3232–3238.
- Palanisamy, A., Salim, N., Parameswaranpillai, J., Hameed, N., 2017. Handbook of Epoxy Blends, pp. 1097–1111.
- Ross, J., 1969. NBS Special Publication No 314, 57-88.
- Shao, Y., Ying, Y., Ping, J., 2020. Chem. Soc. Rev. 49 (13), 4405–4465.
- Shea, A.M., Hammill, B.G., Curtis, L.H., Szczech, L.A., Schulman, K.A., 2008. J. Am. Soc. Nephrol. 19 (4), 764–770.

- Tsunoda, M., Hirayama, M., Tsuda, T., Ohno, K., 2015. *Clin. Chim. Acta* 442, 52–55.
- Urbanowicz, M., Pijanowska, D.G., Jasinski, A., Ekman, M., Bocheńska, M.K., 2019. *J. Solid State Electrochem.* 23 (12), 3299–3308.
- Wang, S., Wu, Y., Gu, Y., Li, T., Luo, H., Li, L.-H., Bai, Y., Li, L., Liu, L., Cao, Y., Ding, H., Zhang, T., 2017. *Anal. Chem.* 89 (19), 10224–10231.
- Wheeler, D.S., Wong, H.R., 2007.
- Whelton, P.K., 2014. *Curr. Hypertens. Rep.* 16 (8), 1–8.
- Williamson, S., Munro, C., Pickler, R., Grap, M.J., Elswick, R.K., 2012. *Nursing Research and Practice* 2012, 246178.
- Xu, J., Murphy, S.L., Kochanek, K.D., Bastian, B., Arias, E., 2018.
- Xu, K., 2021. *J. Micromech. Microeng.* 31 (5), 54001.
- Xu, K., Chen, Y., Okhai, T.A., Snyman, L.W., 2019. *Opt. Mater. Express* 9 (10), 3985–3997.
- Zdrachek, E., Bakker, E., 2018. *Anal. Chem.* 91 (1), 2–26.
- Zimmermann, M., Schmid, H., Hunziker, P., Delamarche, E., 2007. *Lab Chip* 7 (1), 119–125.